CONCRETE RESEARCH LETTERS
www.crl.issres.net
Vol. 5 (1) – March 2014

Strengthening of Concrete Beams Using FRP Composites

Ahmed A. Elshafey[a*], Medhat Mohammed[a],Mostafa M. El-Shami[b], and Kamel S. Kandil[a]

[a] *Department of Civil Engineering, Faculty of Engineering, Menoufyia University, Shebin El-Kom, EGYPT*
[b] *Construction Eng. Dept., University of Dammam, KINGDOM OF SAUDI ARABIA*

ABSTACT

Finite element analysis (FEA) is used to predict the behavior of reinforced concrete beams strengthened with fiber reinforced polymer (FRP). To verify and measure the accuracy of the FEM model, the current model results were compared with both experimental and theoretical available results. Four beams were studied simulating the Horsetail Creek Bridge, Oregon, USA. The first one is a control beam with no strengthening fiber. The second beam is strengthened with carbon fiber reinforced polymer (CFRP) oriented along the length of the beam to reinforce the flexure behavior. The third beam is wrapped with glass fiber reinforced polymer(GFRP) laminates representing the shear beam. The fourth one is strengthened with CFRP and GFRP laminates representing the flexure-shear beam. The load-strain for concrete, steel and fiber as well were represented and compared. In addition, the load deflection curves and crack patterns were developed and represented. The results showed that the modeling process was accurate in simulating the tested beams. It was also clear that using FRP in strengthening reinforced concrete beams is an effective method in improving both shear and flexural behavior of the beams.

Keywords: CFRP; GFRP; Finite element; Strengthening; Concrete; Beam.

1. Introduction

Strengtheningand repairing of concrete elements is widely usedworldwide as the structures deteriorate with time. Some parameters control the use of strengthening technique such as cost and time. Currently, strengthening with FRP is the most common technique used these days.In the past, concrete elements were strengthened by using additional beams, props, or external post-tensioning. However, advances in technology led to the invention of plate bonding technique. Since 1960, retrofitting using steel plates was used around tension face of the elements by using a suitable adhesive. In 1980, FRP proved to be advantageous over steel plates in strengthening several reasons such as its light weight, resistance to corrosion, high strength and stiffness[1].

Various studies have been done on FRP strengthening of concrete elements. Different types of fibers were used such as CFRP, GFRP and Aramid Fiber Reinforced Polymer (AFRP) for repairing in shear [2]. Several researches investigated the effect of environmental condition [3], such as freeze /thaw or wet/dry cycling in a calcium chloride solution. Preparation type and effect of resin type were studied by [4, 5]. Experimental tests were done as well as an analytical models based on Finite Element Method (FEM) [6, 7] using well-known commercial programs as ANSYS [8]. Also, the effect of loading technique (normal loading or cyclic loading) was studied [9]. Most expected failure modes that can be occur were also investigated [1, 3, and 7].

The main objective of this research is to investigate the effect of FRP strengthening of reinforced concrete beams in shear, bending and shear bending using Finite element method (FEM), compare the analytical model results with the experimental results from previous studies to accurately calibrate the model, and study the effect of using GFRP sheets on shear strengthening of reinforced concrete beams.

2. Finite Element Model

2.1 Geometry of tested beams:

Full scale beams were studied with dimension of $305 \times 768 \times 6096\ mm$. The span between the two supports is $5486\ mm$.The distance between the two loads lines is$1829\ mm$as shown in Figure 1. Due to symmetry, one quarter of the full beam was modeled in the FE analysis. It should be noted that these dimensions were chosen to simulate the experimental and theoretical examples [2, 10].

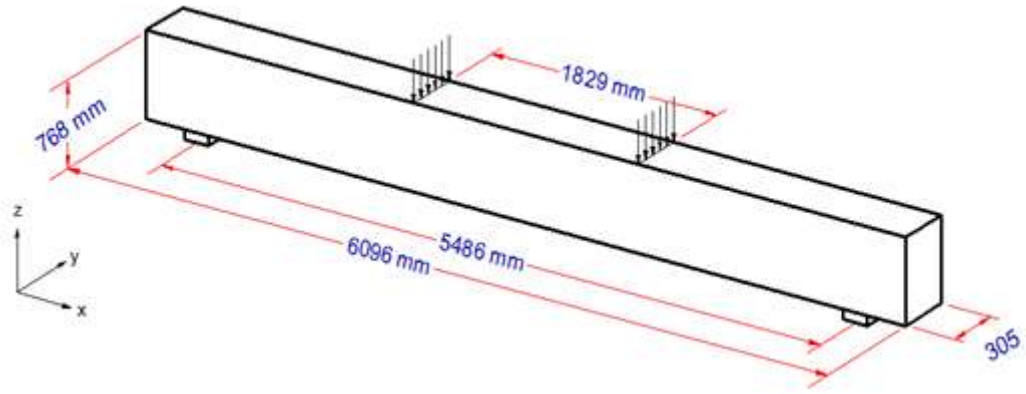

Figure 1: Typical beam dimensions.

Steel reinforcement details for the full-size beams are illustrated in Figure 2. The inclined portions of the steel bars existing in the tested beams were ignored in the FEM for simplicity.

2.2 Finite element modelling(FEM):

Due to symmetry, a quarter of the full beam was modeled. The model is $3048\ mm$ long, with a cross-section of $152.5 \times 768\ mm$.Only one loading plate and one support plate are modeled. In the experiment work, loading and support dimensions were approximately $50.8 \times 203 \times 305\ mm$ and $103 \times 305 \times 25\ mm$,respectively. Beams have been reinforced with various thicknesses of

GFRP and CFRP composites, depending upon the capacities needed at the various locations on the beams. The use of fibers with various thicknesses creates discontinuities, which are not desirable in the FE analysis. To overcome that, a constant overall thickness of FRP composite was used in the models. To keep the model equivalent, overall stiffness of the FRP materials, the elastic and shear modulus assigned to each FRP layer were modified to achieve the overall stiffness such as:

$$G_{xy} = \frac{E_x E_y}{E_x + E_y + 2\upsilon_{xy} E_X} \quad (1)$$

where,

G_{xy} is the shear modulus in the *xy*-plane,

E_x isthe elastic modulus in the *x*-direction,

E_y is the elastic modulus in the *y*-direction, and

υ_{xy} ispoison's ratio in the *xy*-plane.

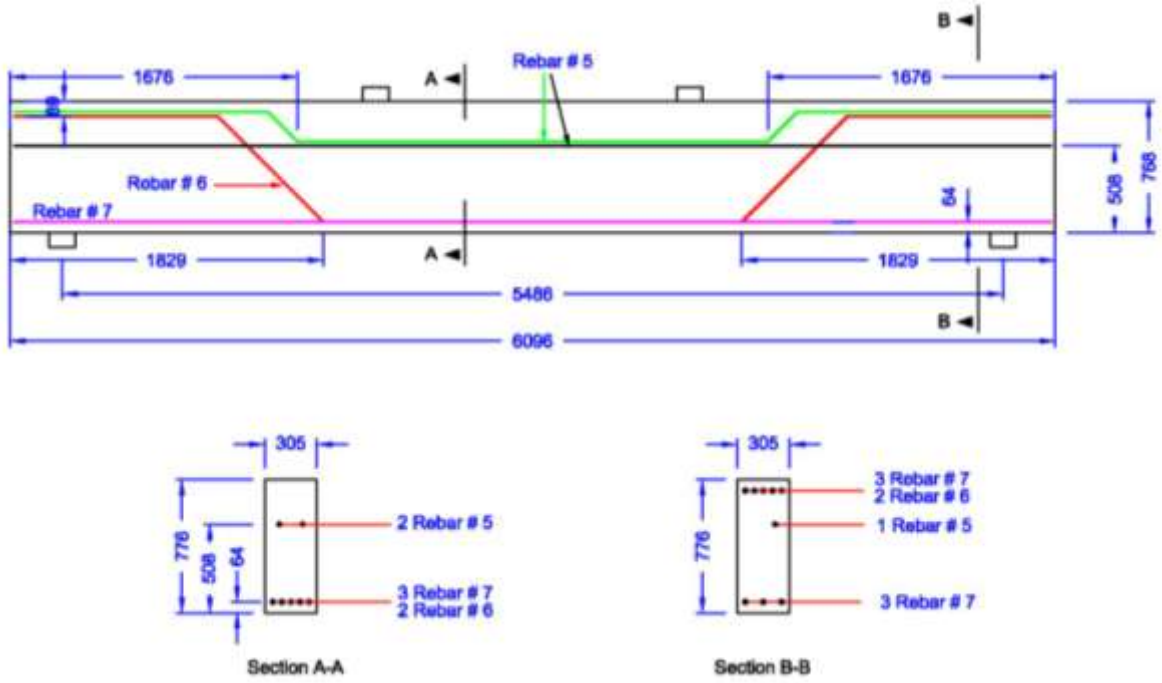

Figure 2: Typical steel reinforcement locations [8].

In FE analysis, some modifications of dimensions were done due to geometry, element connectivity, meshing of concrete and steel locations. Figure 3 shows the modified dimensions of the FRP reinforcing schemes for the quarter beam models.

2.3 Elements types used in modelling:

ANSYS, 2007 includes a lot of elements which differ in properties, geometry, and degrees of freedom. The elements used in this research were:

- Solid element, SOLID65 was used for the concrete.
- Solid element, SOLID45 was used for steel plates at supports and loading area.
- Link element, LINK8 was used for steel rebar.

- Shell element, SHELL41 was used for FRP sheets.

To complete mesh attributes material number and real constant must be defined. Material numbers assigned the material properties. Real constant assigned the cross section properties.

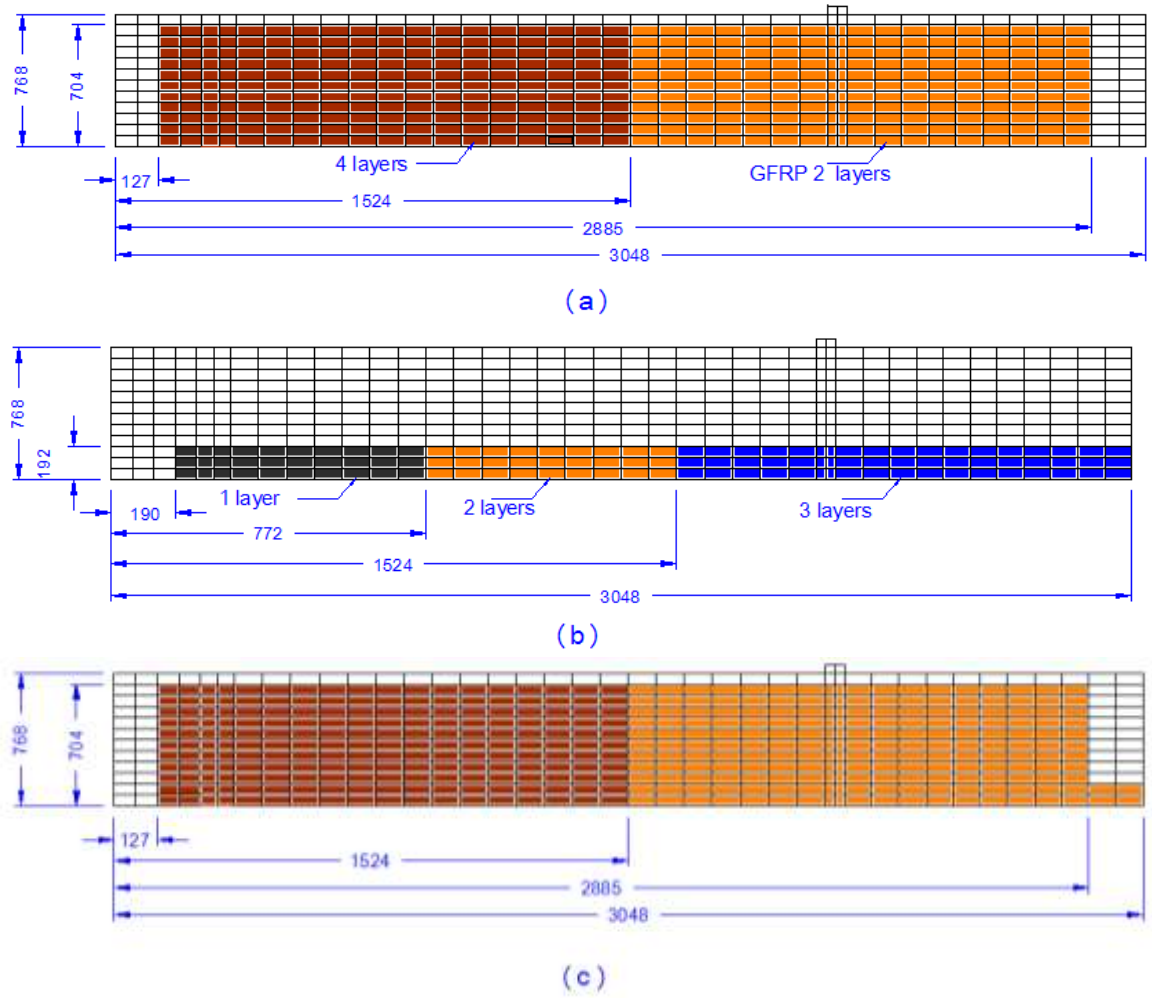

Figure 3: Modified dimensions of FRP reinforcing for strengthened beam models
(a) Shear Beam; (b) Flexure Beam; (c) Flexure-Shear Beam.

2.4 Reinforced concrete:

SOLID65 was used for modeling concrete. SOLID65 is capable of cracking in tension and crushing in compression. The eight-node element has three degrees of freedom at each node. The degrees of freedom are translations in the nodal X, Y, and Z directions. The most important aspect for this element is the treatment of nonlinear material properties. The concrete is capable of cracking (in three orthogonal directions), crushing, plastic deformation, and creep. SOLID65 element is shown in Figure 4.

2.5 Steel rebar:

The 3-D spar element LINK8 was used to model the steel reinforcement. LINK8 is a two-node element having three degrees of freedom at each node; translations in the nodal X, Y, and Z

directions. The element is also capable of plastic deformation, creep, swelling, stress stiffening, and large deflection capabilities. Figure 5 illustrates the geometry and node locations for this element type.

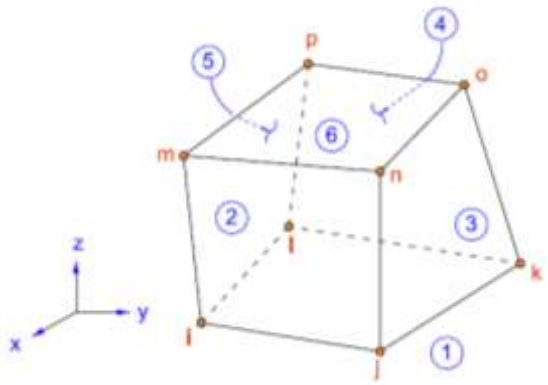

Figure 4: Solid65 3-D reinforced concrete solid element.

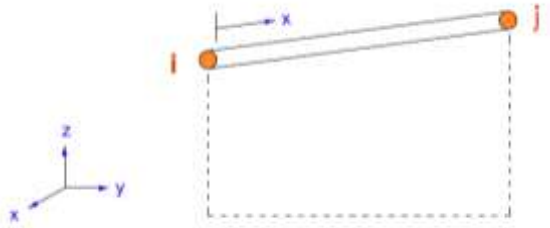

Figure 5: LINK8 3-D spar.

2.6 FRP composites:

SHELL41 element was employed to model the FRP composites; it is a 3-D element having membrane (in-plane) stiffness but no bending (out-of-plane) stiffness. It is intended for shell structures where bending of the elements is of secondary importance. The element has three degrees of freedom at each node; translations in the nodal X, Y, and Z directions. The geometry, node locations, and the coordinate system are shown in Figure 6.

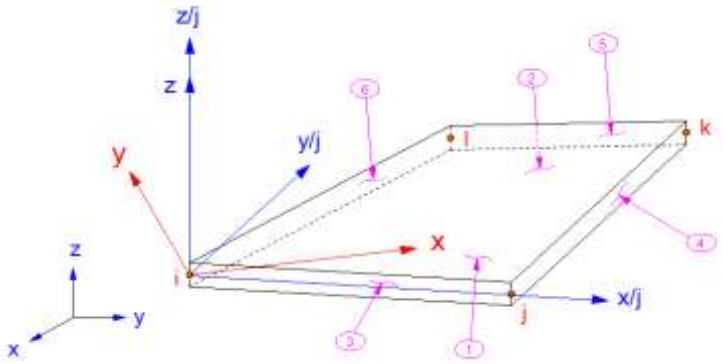

Figure 6: SHELL41 geometry and coordinate system.

2.7 Bond between elements

Perfect bond between elements was assumed. The link element for the steel reinforcing (LINK8) was connected between nodes of each adjacent concrete solid element (SOLID65). The same approach was adopted for FRP composites as shown in Figure 7. The perfect bond assumption achieved using the high strength of the epoxy or by mechanical anchors used to attach FRP sheets to the experimental beams.

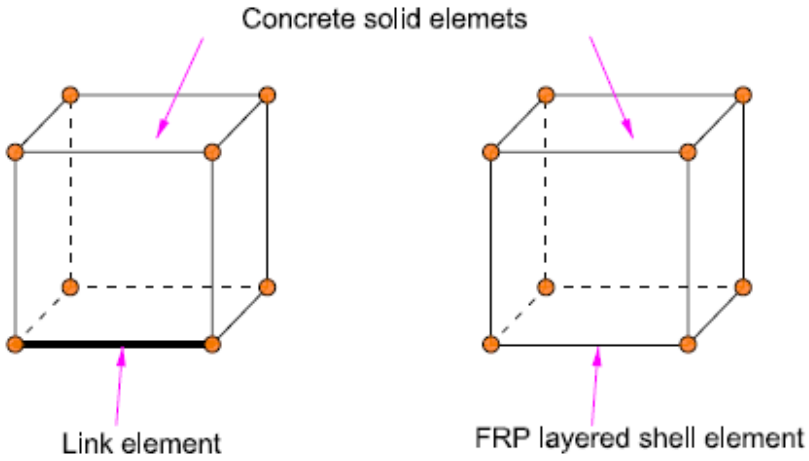

Figure 7: Element connectivity: (a) Concrete solid element and link element;
(b) Concrete solid element and FRP layered shell elements.

2.8 Supports and loading plates:

SOLID45 element was chosen to model steel plates at the supports and load application on the beam. The element is defined by eight nodes having three degrees of freedom at each node; translations in the nodal X, Y, and Z directions. The element has plasticity, creep, stress stiffening, large deflection, and large strain capabilities. The nodes location, geometry, and coordinate system are shown in Figure 8.

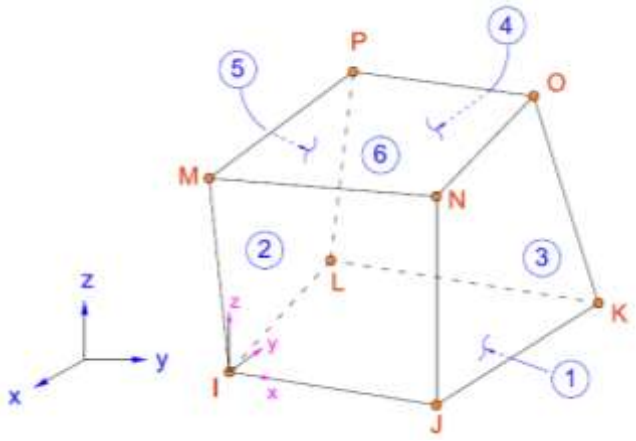

Figure 8: SOLID45 3-D solid element (ANSYS, 2007).

3. Material Properties:

3.1. ***Concrete:***

Implementation of concrete properties in the model was a challenging task. Concrete has different behavior in tension and compression. Properties of concrete elements are shown in Table 1.

TABLE 1: SUMMARY OF MATERIAL PROPERTIES FOR CONCRETE

Beam	E_C (MPa)	$f_c^{\backslash}$ (MPa)	f_r (MPa)	υ
Control beam	1.930E+07	16708.75	2545.61	0.2
Flexure beam	1.758E+07	13744.98	2309.05	0.2
Shear beam	1.813E+07	14723.13	2389.58	0.2
Flexure-shear beam	1.758E+07	13744.97	2309.05	0.2

Stress-strain relationship for concrete in compression is important in FEM. It was obtained using numerical expressions (Desayi and Krishnan, 1964) and simplified as shown in Figure 9.

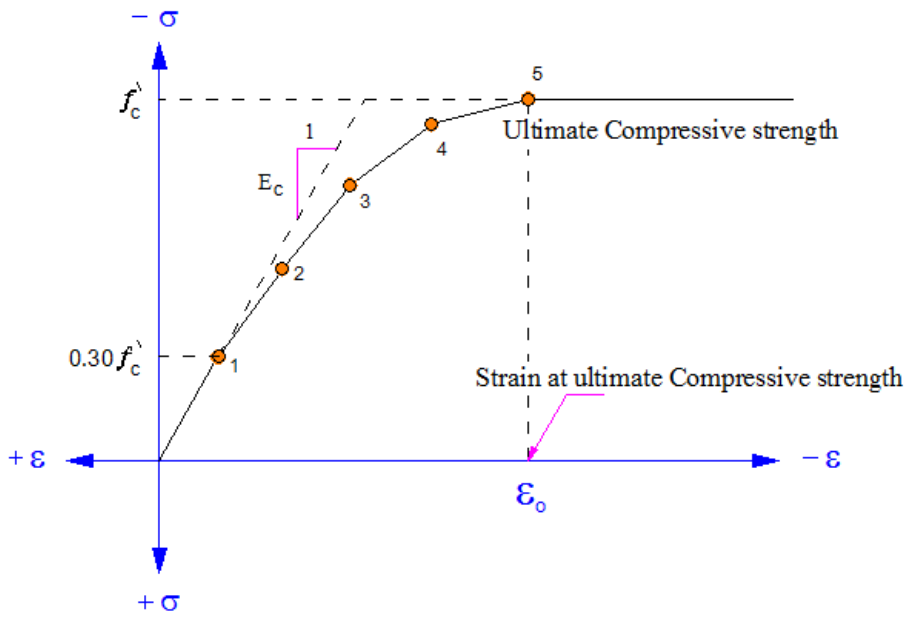

Figure 9: Compressive uniaxial stress-strain curve for concrete (Kachlakev et al. 2001) [11].

3.2. ***Steel reinforcement and steel plates:***

The element LINK8 refers to all the steel reinforcement in the beams. The properties of steel used in the model are the same as the experimental investigation (Kachlakev and McCurry,

2000)[2]. The steel for the FEM was assumed to be bilinear isotropic. Material properties for the steel used in all models are shown in Table 2.

Element SOLID45 was used to model steel plates at support locations and loading points to avoid more stress concentration over the support areas and loading points. This element is modeled as a linear isotropic element.

TABLE 2: SUMMARY OF MATERIAL PROPERTIES VALUES FOR STEEL REINFORCED THE BEAM.

Properties	Steel reinforcement	Steel plate
E_s	199948 (MPa)	199948 (MPa)
f_y	413685 (MPa)	*
υ	0.3	0.3

* The stress strain curve of steel plate was considered as linear.

3.3. FRP Composites:

FRP composites are composed of resins, reinforcements, fillers, and additives. Each of these constituent materials or ingredients plays an important role in the processing and final performance of the end product. FRP composites are anisotropic (non-uniform properties in all directions).

FRPs were simulated as orthogonalmaterial that has three planes XY, XZ, and YZ. The XYZ coordinate axes are the principal coordinates for fibers. Local coordinate system is very important and is needed to define the FRP shell elements correctly. The X axis was in the same direction as the fiber direction. The Y axis was the direction of the width of the fiber while the Z axis was perpendicular over the other axis. In this article, the FRP composites properties were chosen to be the same in both of Y and Z directions. A summary of material properties of FRP used for the modeling of all three beams is shown in Tables 3 and4.

TABLE 3: SUMMARY OF MATERIAL PROPERTIES VALUES FOR CFRP.

FRP	Property	One layer	Two layers	Three layers
CFRP with thickness 1.016 mm	E_x (MPa)	62053	124106	186158
	E_y (MPa)	4826	9652	14478
	E_z (MPa)	4826	9652	14478
	υ_{xz}	0.22	0.22	0.22
	υ_{xy}	0.22	0.22	0.22
	υ_{yz}	0.3	0.3	0.3
	G_{xz} (MPa)	3268	6536	9804
	G_{xy} (MPa)	3268	6536	9804
	G_{yz} (MPa)	1861	3722	5583

3.4.Loading and Boundary Conditions:

The same locations of support and loading plates were considered as the full-size beams. The experimental steel plate dimensions for support were $4" \times 12" \times 1"$, and for loading $2" \times 8" \times 12"$. The steel plate was added to avoid stress concentration at the support and loading locations. The support was modeled as a roller support and hinged constraint at a one line of nodes under the plate

in the Y, and Z directions. Also the load applied vertically on center line of plate. Figure 10 illustrates the plate and applied loading.

TABLE 4: SUMMARY OF MATERIAL PROPERTIES VALUES FOR GFRP.

FRP	Properties (psi)	Two layers	Four layers
GFRP with thickness 1.27 mm	E_x (MPa)	41368	82737
	E_y (MPa)	13789	27579
	E_z	13789	27579
	υ_{xz}	0.26	0.52
	υ_{xy}	0.26	0.52
	υ_{yz}	0.3	0.6
	G_{xz} (MPa)	3034	6068
	G_{xy} (MPa)	3034	6068
	G_{yz}	5309	10618

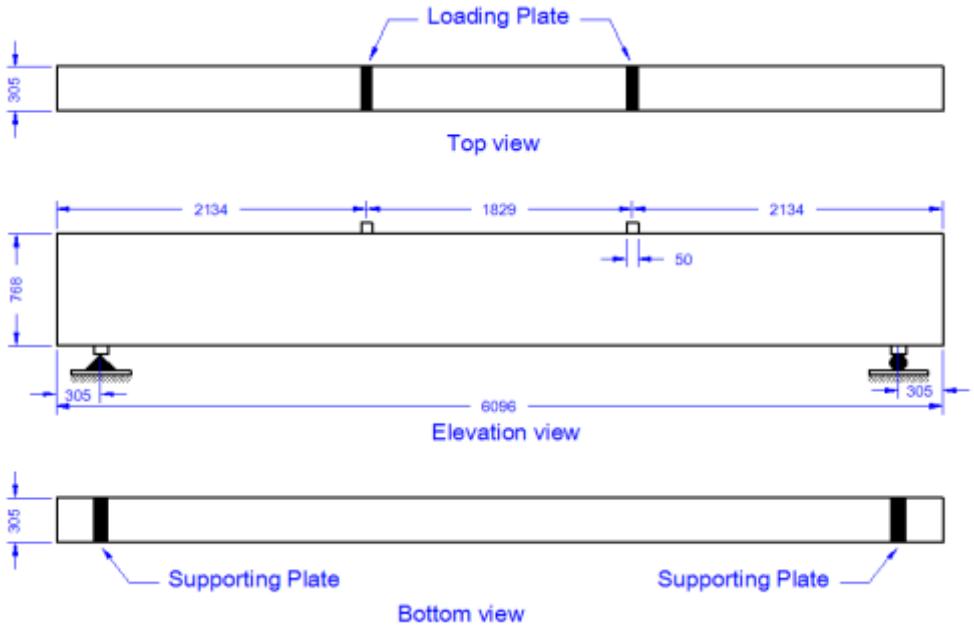

Figure 10: Loading and support locations (McCurry and. Kachlakev, 2000).

Symmetry conditions allowed a quarter of the beam to be modeled. Constrains are applied at symmetry planes in the direction perpendicular to the plane of symmetry. At plane of symmetry parallel to YZ plane, U_x is equal to zero and at plane parallel to XZ, U_Y is equal to zero.

3.5.Solution control and analysis of the model:

In this research static analysis was used for finite element model of simply supported beam under vertical loading. To preform solution at a specific range of load, load steps, sub steps were applied using do loops. Data were recorded every load step to show all trackedparameters and to decrease the storage volume of recorded data. If results were recorded every sub step, it will need very large desk space. Sub steps option was used to overcome the conversion difficulties. Do-loop command was used to control the conversion issue and to decrease the time required for solution. It

should be noted that the time needed in the (Kachlakev and McCurry, 2001) was around 120 hours for solution the model but with the current research the run time was reduced to less than 1 hours.

4. Results From FEM of Full-Size Beams:

Results from the finite element analysis are compared with the experimental data for the full-size beams and with the theoretical results obtained in this research [1, 2]. The following comparisons are made:

- Load-strain plots at selected locations,
- Load-deflection plots at mid-span,
- First cracking loads, loads at failure and crack patterns at failure.

The data obtained from the theoretical analysis are at the same location of strain gauges used in experimental tests as shown in Figure 11.

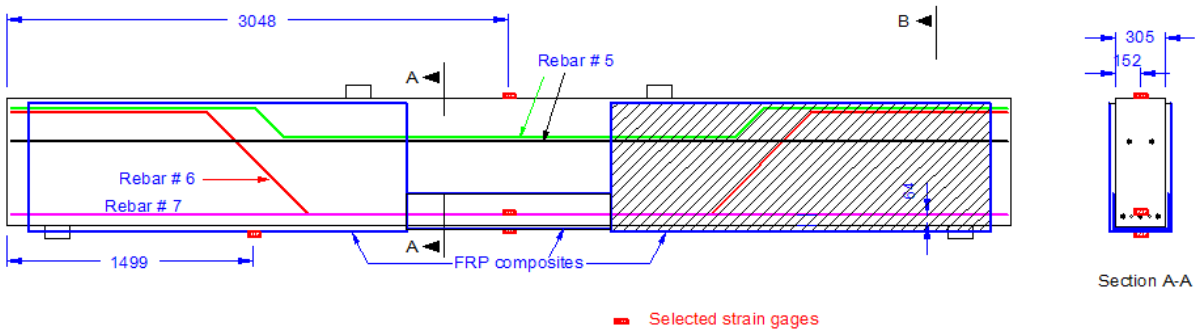

Figure 11: Selected strain gauge locations (not to scale) (McCurry and Kachlakev, 2000).

4.1.Load-Strain Plots:

4.1.1. Tensile strain in lower steel reinforcing:

In Experimental beams strain data were collected using strain gauges fixed on steel bar # 7 at the mid-span of control, flexure, and shear beams. For flexure-shear beams, data were collected for steel bar # 6 at mid-span (see Figure 11). The comparison between the total load and strain on bar #7 from finite element analysis and the experimental work are shown in Figures12 to 15.

It can be seen from these figures that the relationship between load and strain for main steel in current research was in good agreement with experimental results and theoretical results [1,2] in linear strain portion and little deviation afterword. In the experimental beams, concrete at the first crack can resist amount of tension but in the finite element model the stiffness decrease to zero, therefore the tension in steel element does not change as in experimental beams. Strains from FE were higher than experimental results (McCurry and Kachlakev, 2000) [2].

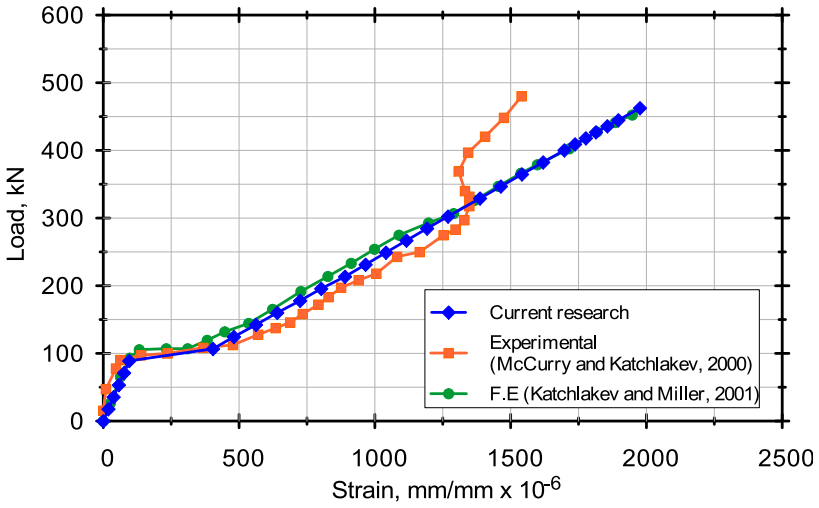

Figure 12: Load-strain curve for steel bar # 7 in the control beam.

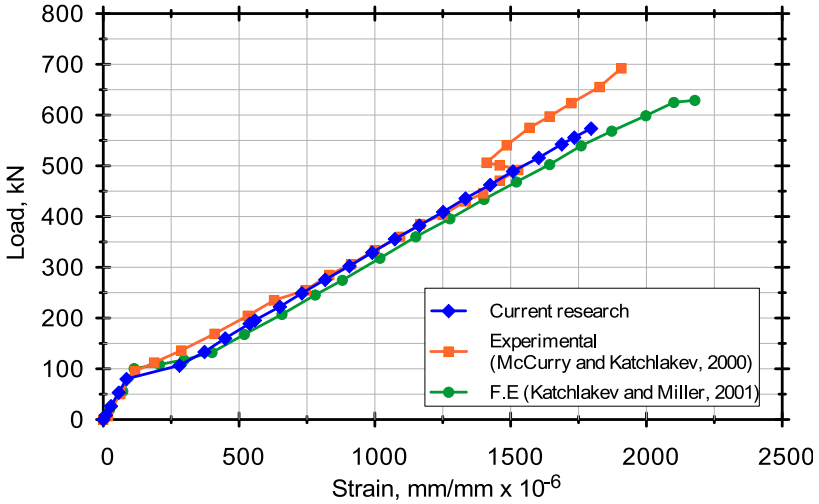

Figure 13: Load-strain curve for steel bar # 7 in flexure beam.

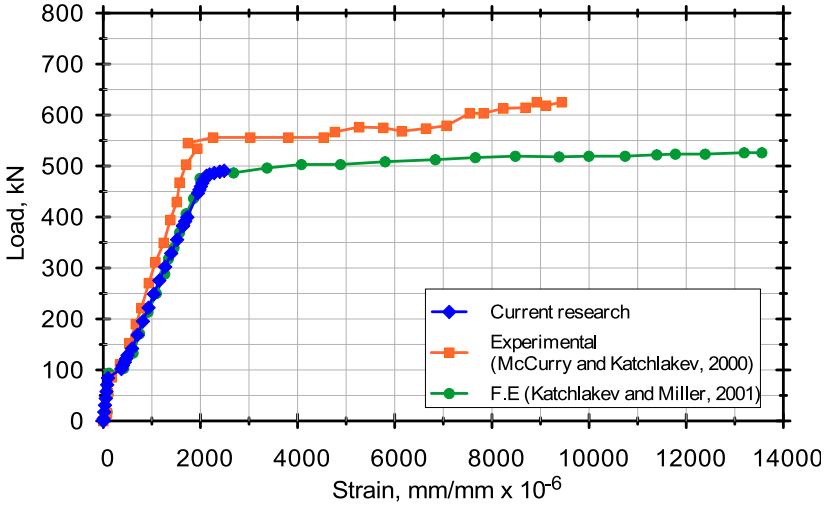

Figure 14: Load-strain curve for steel bar # 7 in shear beam.

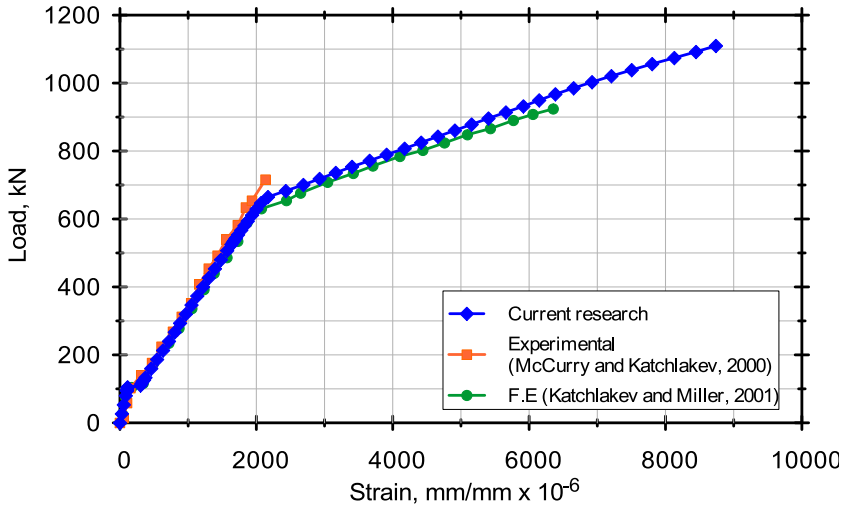

Figure 15: Load-strain curve for steel bar # 6 in flexure-shear beam.

4.1.2. Compressive strain in concrete:

Strain gauge was placed at mid-span on the top face for beams as shown in Figure 14. Comparison was made between the experimental results and FE analysis of previous research and current research for four beams tested and shown in Figures16 to 19.

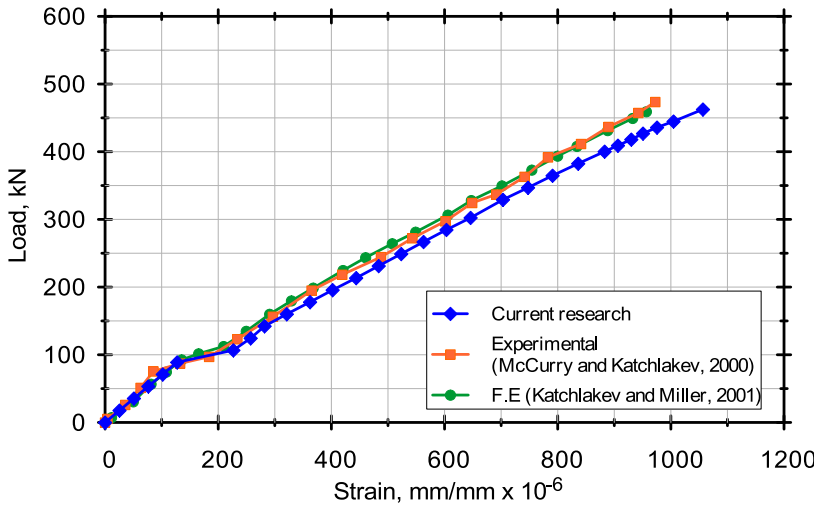

Figure 16: Load-compressive strain curve for concrete in control beam.

In brief the four Figures from Figures 16 to 19 compressive strain curves for concrete have some difference between the experimental results and finite element result. This may be attributed to a mistake in calibration or in fixing the strain gages or a defect in the material of the concrete beams.

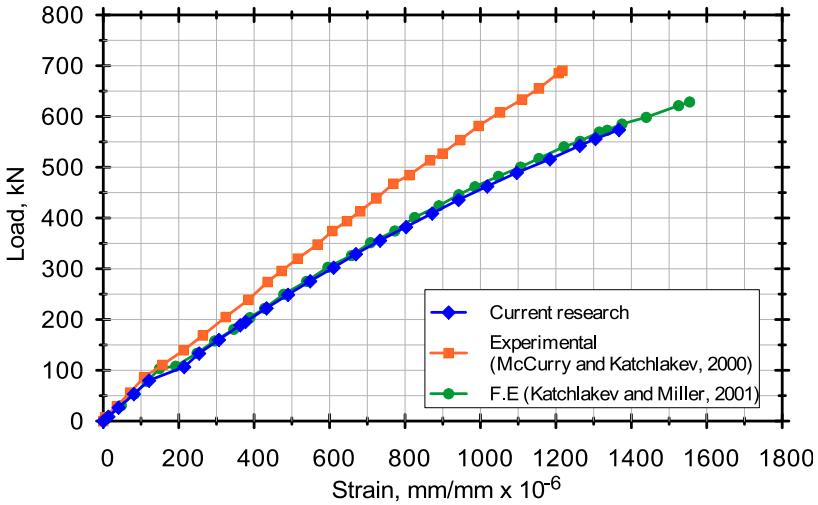

Figure 17: Load-compressive strain curve for concrete in flexure beam.

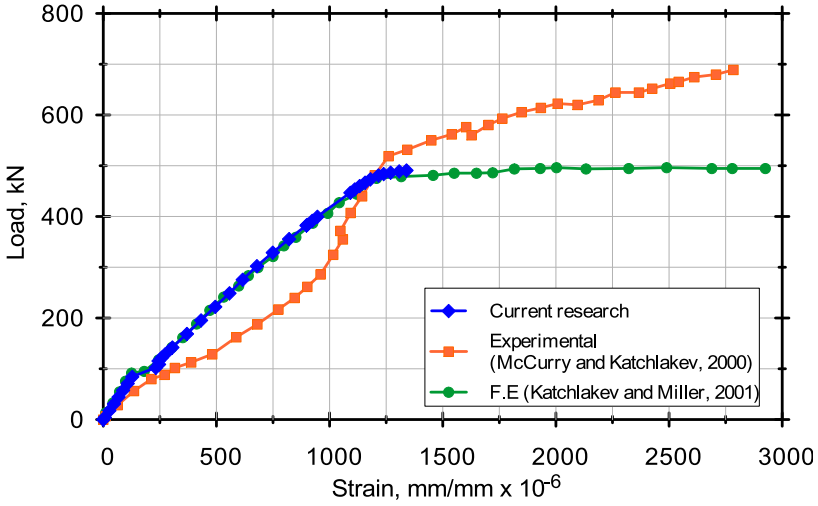

Figure 18: Load-compressive strain curve for concrete in shear beam.

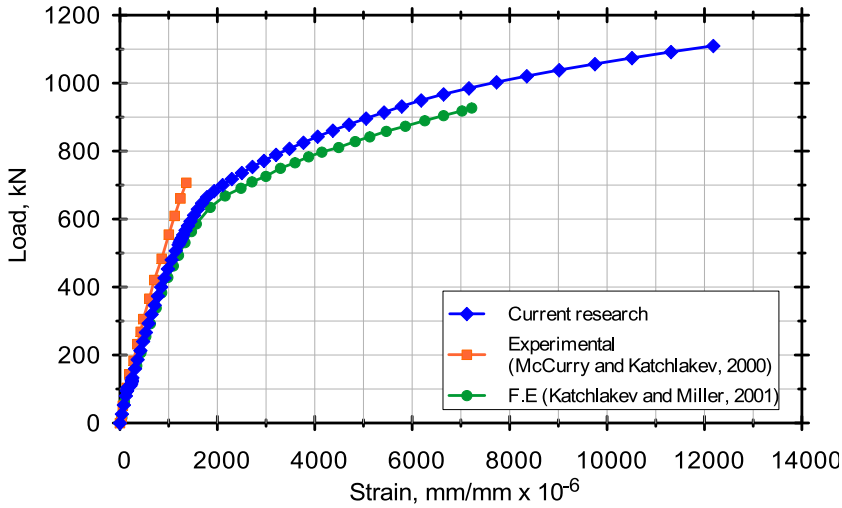

Figure 19: Load-compressive strain curve for concrete in flexure-shear beam.

4.1.3. Tensile Strain in FRP Composites:

Strains in FRP composites were measured at the bottom of the beam at mid-span on the surface of the CFRP composite as shown Figure 11. For the shear beam the strain was collected from the bottom of the beam at 59 in far from the end of the beam. Comparisons of the total load on the beam with strain in FRP collected from experimental results and previous FE analysis and current research are shown from Figures20 to 22.

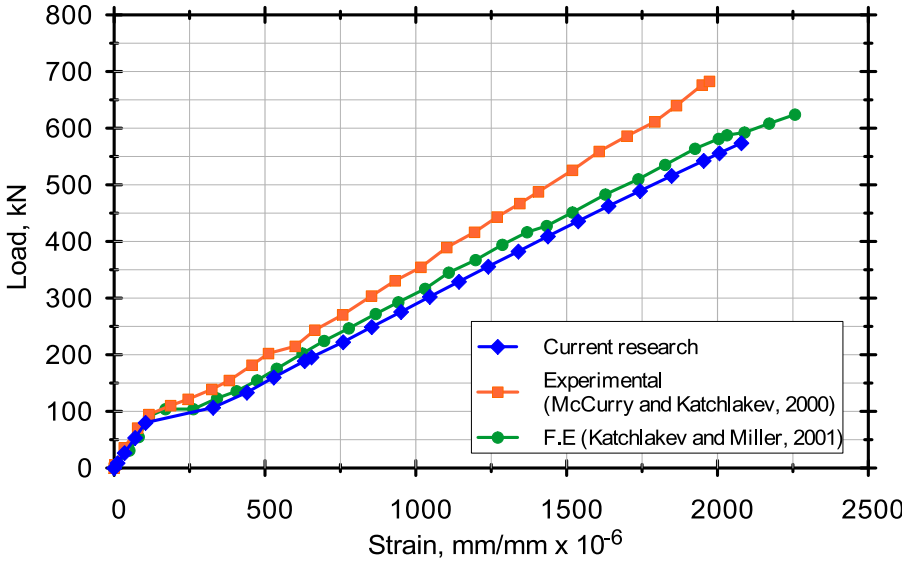

Figure 20: Load strain curve in the CFRP for the flexure beam.

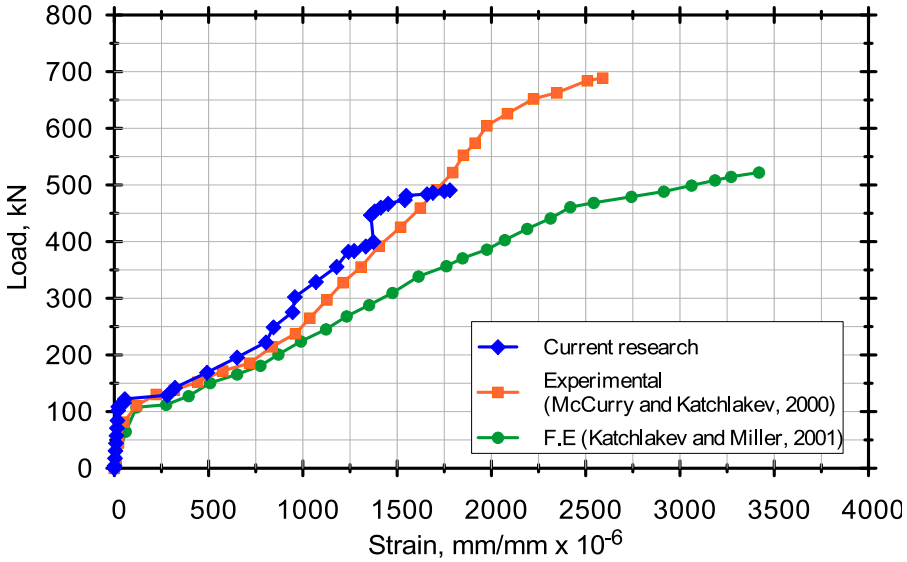

Figure 21: Load strain curve in the GFRP for the shear beam.

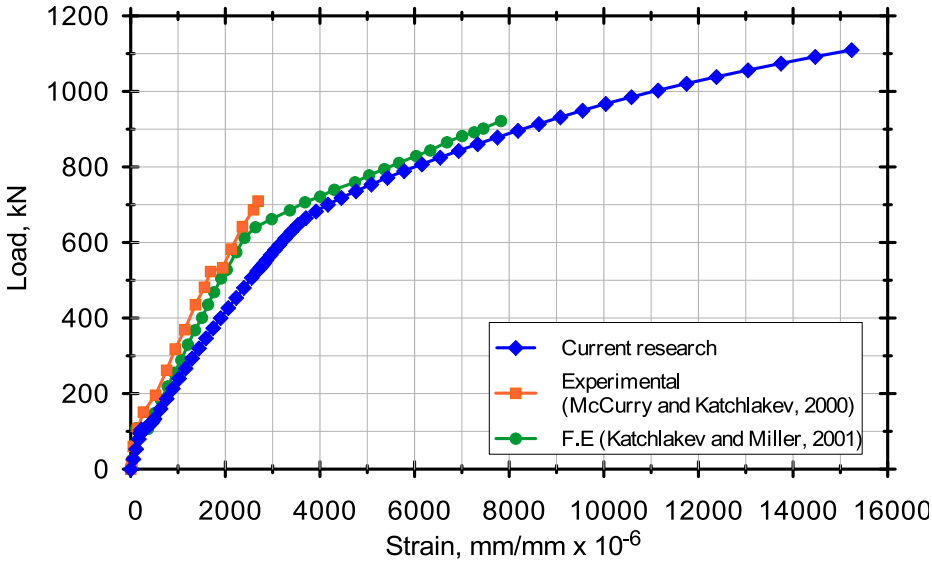

Figure 22: Load strain curve in the CFRP for the flexure-shear beam.

From the previous figures from 20to 22 for relationship between load and strain results get good agreement with experimental. Also the strain obtained from the current research in GFRP for shear beam gets good agreement with experimental and better results than those of the FE by (Kachlakev and Miller, 2001)[11].

4.2. Loads-deflection relationship:

The deflection measured at center point at mid-span of each beam. The deflection data collected from FE in current study was measured at the same location of the experimental beam. The comparison for load deflection curve from experimental result and previous analytical research and current research using FE are shown in Figures23 to 26.

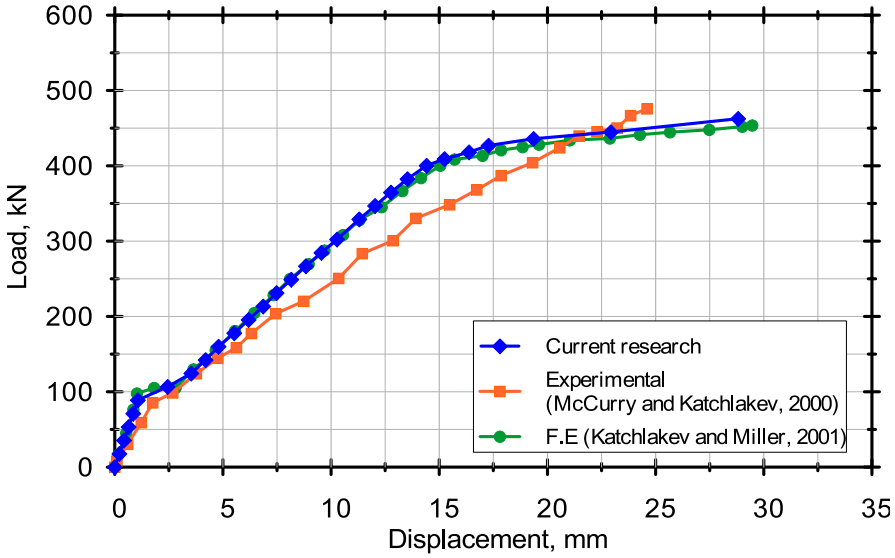

Figure 23: Load-displacement curve for control beam.

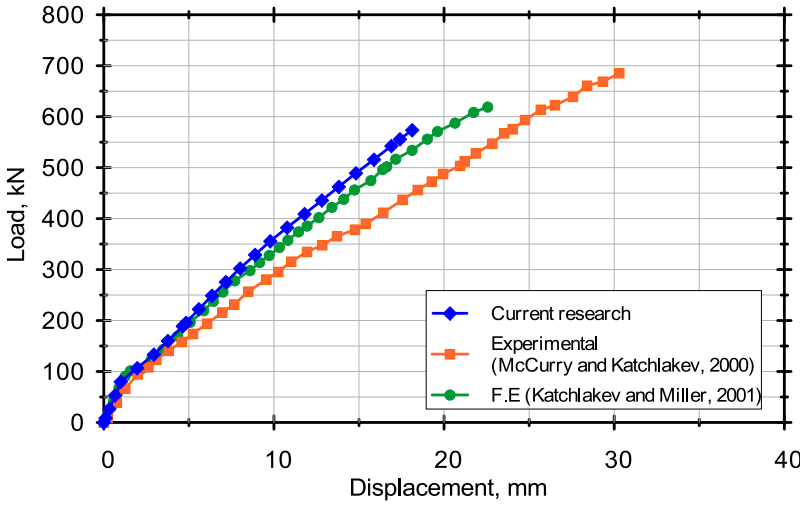

Figure 24: Load-displacement curve for flexure beam.

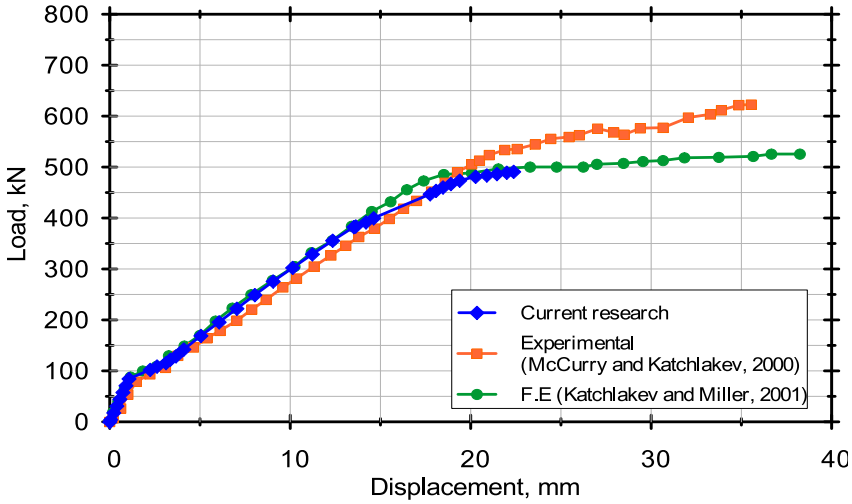

Figure 25: Load-displacement curve for shear beam.

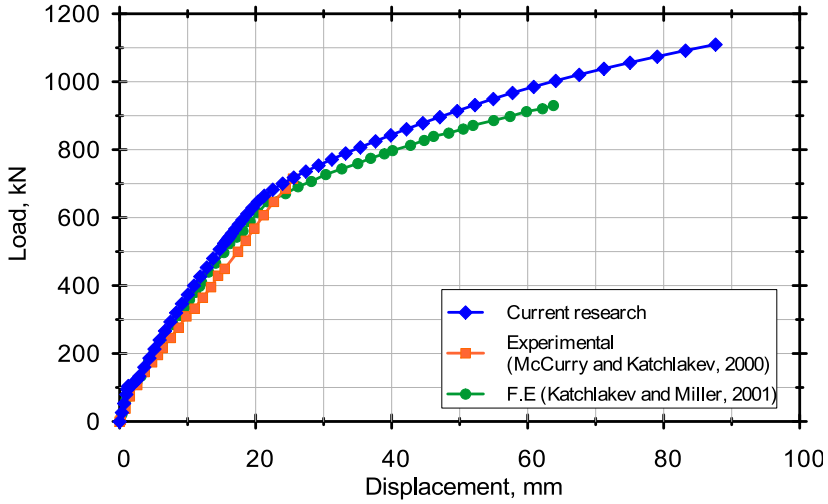

Figure 26: Load-displacement curve for flexure-shear beam.

Finally, the load deflection relationship for the four beams indicates good agreement between the experimental results and the finite element results with some different. Some factors can lead to this difference as micro cracks formed during drying which reduce the stiffens of the tested beams also in finite element model the bond between the concrete and the steel are fully bonded but in the actual beam there is some slip between the bars and the concrete during the nonlinear behavior (Kachlakev et al. 2001) [11].

4.3. Loads-Deflection of the Studied Beams Using FEM:

Figure 27 shows the load deflection relationship between the four beams solved by FE. The curves indicated that in the linear part the stiffness of beams for control beams and strengthened beams are the same. But after that the beams strengthening with FRP get high stiffness than the control beams.

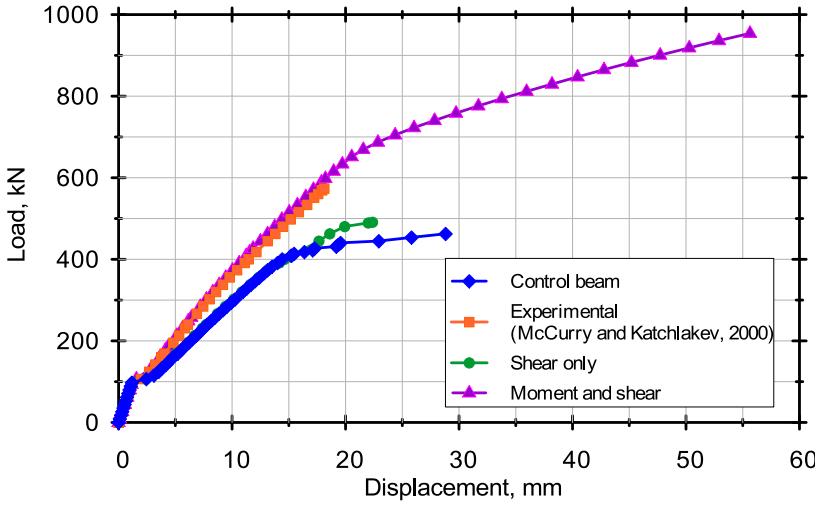

Figure 27: Load-displacement curves for the studied beams solved by FEM.

4.4. Crack Patterns for the Studied Beams:

ANSYS permits to see the crack pattern in different load steps until failure. The crack appears when the tensile stress reaches the ultimate stress. The cracks are drawn as small circles and take direction perpendicular to the direction of the principle stress. The crack pattern is shown in Figures 28 to29 (a, b, c, d).

5. CONCLUSIONS AND RECOMMENDATIONS:

In this research a FEM using ANSYS program is used to predict the behavior of reinforced concrete beams strengthened with FRP. Comparison between pervious experimental results (Kachlakev and McCurry, 2000) and theoretical results (Kachlakev and Miller, 2001) with the current results was conducted. Four beams were studied simulating the Horsetail Creek Bridge. The first one is a control beam with no fiber. The second one is strengthened with CFRP oriented along the length represents the flexure beam. The third one is wrapped with GFRP laminates represents the shear beam. The fourth one is strengthened with CFRP and GFRP laminates represents the flexure-shear beam. The results were represented in load-strain plots for concrete, steel and fiber. In addition, the load deflection curves and crack patterns were also represented. The results showed that the modeling process was accurate in simulating the tested beams. It was also clear that using

FRP in strengthening reinforced concrete beams is an effective method. The following conclusions are drawn from this study:

1) A comparison between the previous experimental and theoretical results with this research was done. The results showed good agreement between previous researches and the current research.
2) The current model proofed to be a good technique that can be used to produce acceptable theoretical results with ease in application.
3) The previous researchers simulate the fiber in ANSYS program using solid element. But, in this research shell element were used in simulating fiber. Using shell element is more accurate in simulating the actual case than solid element.
4) From the current results it was clear that strengthening of beams in shear using strips of fiber or with continuous sheets did not show much difference.
5) Usually most of researchers enter data to ANSYS using the direct plotting method. This technique is difficult in entering data also in making any modification or discovering any errors. For this reason a subroutine was introduced through which the user can enter the data and change it in a more efficient way.

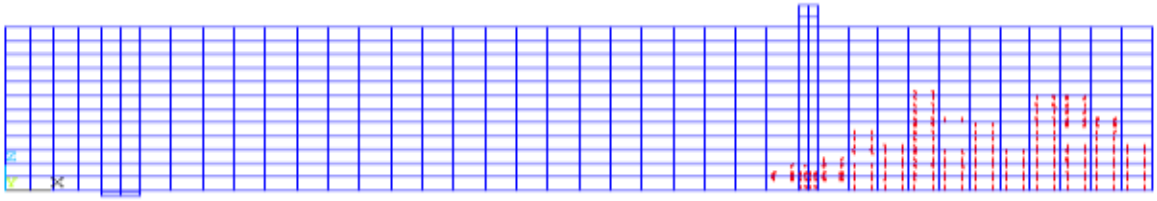

(a)

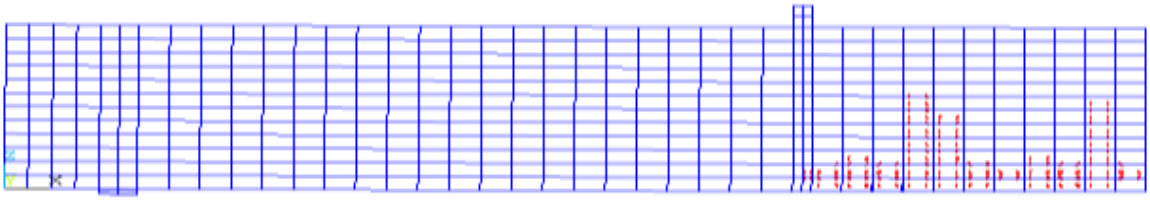

(b)

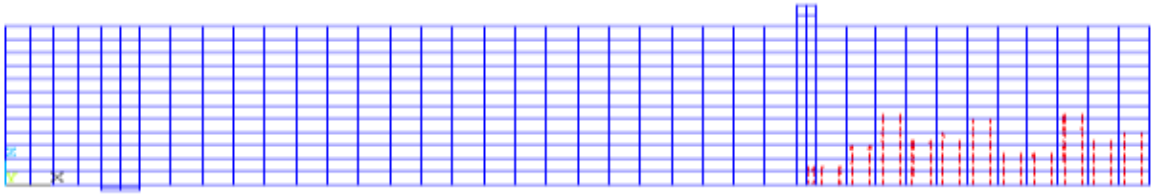

(c)

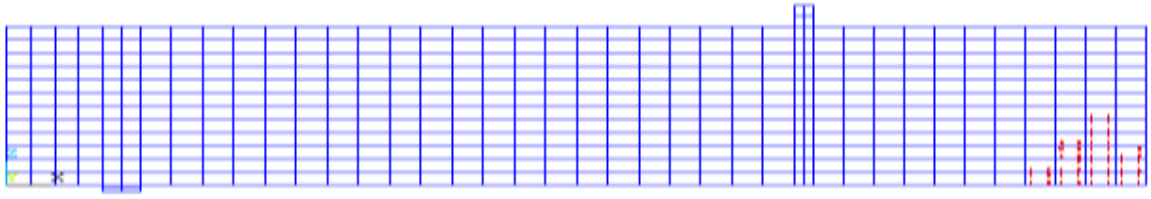

(d)

Figure 28: (a) crack pattern for control beam at first crack (24 kips); (b) crack pattern for shear strengthening beam at first crack (22.5 kips); (c) crack pattern for flexure strengthening beam at first crack (24 kips); (d) crack pattern for flexure-shear strengthening beam at first crack (24 kips).

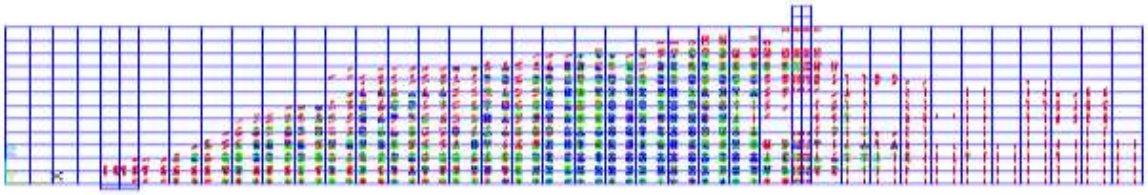

(a)

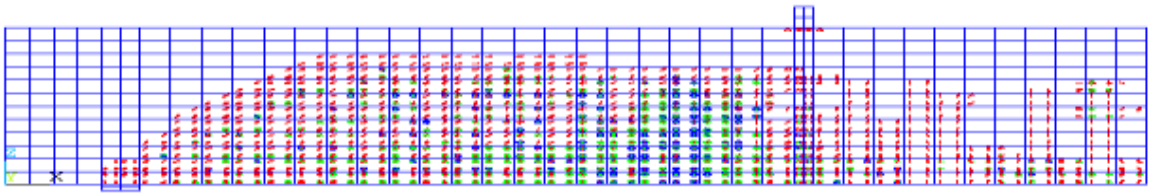

(b)

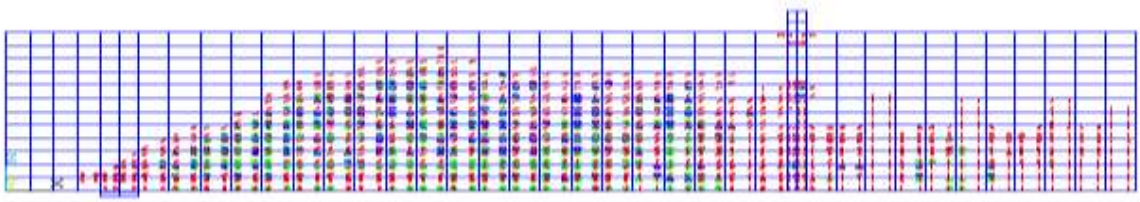

(c)

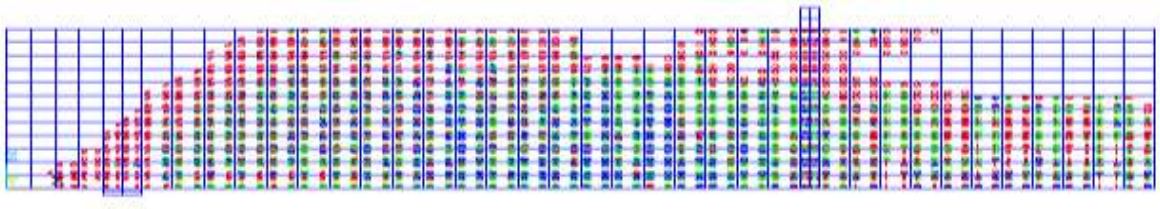

(d)

Figure 29: (a) crack pattern for control beam at load 104 kips; (b) crack pattern for shear strengthening beam at load 110 kips; (c) crack pattern for flexure strengthening beam at load129 kips; (d) crack pattern for flexure-shear strengthening beam at load 249.5 kips.

6. REFERENCES:

[1]Abdel-Jaber, M.S., Walker, P.R., and Hutchinson, A.R. (2003), Shear Strengthening of reinforced concrete beams using different configurations of externally boned carbon fibre reinforced plate. Materials and Structures, Vol. 36, pp 291-301.

[2][Kachlakev, D., and McCurry, D.D., (2000), "Behavior of full-scale reinforced concrete beams retrofitted for shear and flexural with FRP laminates," Composites: Part B, 31, pp. 445-452.

[3]Chajes, M.J., Thomson, T.A., Farschman, J.A., and Farschman, C.A., (1995), "Durability of concrete beams externally reinforced with composite fabrics," Construction and Building Materials, Vol. 9, No. 3, pp. 141-148.

[4]Gao, B., Kim, J.-K., and Leung, C.K.Y., (2004), "Experimental study on RC beams with FRP strips bonded with rubber modified resins," Composites Science and Technology, 64, pp. 2557–2564.

[5]Toutanji, H., and Ortiz, G., (2001), "The effect of surface preparation on the bond interface between FRP sheets and concrete members," Composite Structures, 53, pp. 457-462.

[6]Obaidat, Y.T., Heyden, S., and Dahlblom, O., (2010), "The effect of CFRP and CFRP/concrete interface models when modeling retrofitted RC beams with FEM," Composite Structures, 92, pp. 1391–1398.

[7]Yang, Z.J., Chen, J.F., and Proverbs, D., (2003), "Finite element modelling of concrete cover failure in FRP plated RC beams," Construction and Building Materials, 17, pp. 3–13.

[8]Hawileh, R.A., Naser, M., Zaidan, W., and Rasheed, H.A., (2009), "Modeling of insulated CFRP-strengthened reinforced concrete T-beam exposed to fire," Engineering Structures, 31, pp. 3072-3079.

[9]Capozucca, R., and Cerri, M. N., (2002), "Static and dynamic behaviour of RC beam model strengthened by CFRP-sheets," Construction and Building Materials, 16, pp. 91-99.

[10] Perera, R., Barchín, M., Arteaga, A., and De Diego, A., (2010), "Prediction of the ultimate strength of reinforced concrete beams FRP-strengthenedin shear using neural networks," Composites: Part B, 41, pp. 287–298.

[11] Kachlakev, D., Miller, T., Yim, S., Chansawat, K. and Potisuk, T. (2001). "Finite Element Modeling of Concrete Structures Strengthened with FRP Laminates," Final Report, SPR 316, Report No. FHWA-OR-RD-01-17, for Oregon Department of Transportation, Salem, OR, and Federal Highway Administration, Washington, DC, May 2001, 111 pp.